JOURNAL OF MATERIALS SCIENCE 21 (1986) 1967–1973

Reactions in the formation of $Na_3Zr_2Si_2PO_{12}$

V. A. NICHOLAS, A. M. HEYNS*, A. I. KINGON, J. B. CLARK
National Institute for Materials Research, Council for Scientific and Industrial Research, Pretoria, Republic of South Africa
**Department of Chemistry, University of Pretoria, Republic of South Africa*

Nasicon ceramics of formula $Na_3Zr_2Si_2PO_{12}$ were prepared from two systems, namely $NH_4H_2PO_4$–Na_2CO_3–SiO_2–ZrO_2 and Na_3PO_4–SiO_2–ZrO_2. The partial reactions and sequence of reactions was studied using differential thermal analysis and X-ray diffraction analysis. Kinetic restraints to completeness of reaction are indicated and sodium oxide volatilization is shown to occur. The rate-determining partial reaction involves zirconia and a sodium phosphosilicate intermediate.

1. Introduction

A family of Nasicon solid electrolytes of general composition $Na_{1+x}Zr_2Si_xP_{3-x}O_{12}$ (with $0 \leqslant x \leqslant 3$) were first identified by Hong [1] as possible substitutes for the beta″-aluminas. Nasicon compositions that exhibit the highest ionic conductivities lie within the range $1.8 \leqslant x \leqslant 2.4$ [2–5].

A recurring problem in the fabrication of Nasicon electrolytes is the presence of free zirconia in the final sintered ceramic [3, 6, 7]. The presence of ZrO_2 may arise from three sources: incomplete reaction of the raw materials, the volatilization of sodium oxide during firing [8] and decomposition of intermediates of reaction or of Nasicon itself [9]. This paper is directed toward the understanding of the partial reactions leading to the formation of Nasicon of formula $Na_3Zr_2Si_2PO_{12}$ from two starting systems, namely a four–component system comprised of $NH_4H_2PO_4$, Na_2CO_3, quartz and ZrO_2 and a three–component system comprising Na_3PO_4, quartz and ZrO_2. Particular attention is given to the formation of intermediates that either facilitate or inhibit reaction.

2. Experimental Methods

Raw materials used were reagent grade quartz, Selectipur ZrO_2 and analytical grade Na_2CO_3 and $NH_4H_2PO_4$. The Na_3PO_4 used in the three-component system was prepared using the procedure of Porthault and Merlin [10].

Differential thermal analysis (DTA) studies were conducted on the raw materials and on appropriate stoichiometric binary, ternary and quaternary combinations of the raw materials. The studies were conducted on a Du Pont 1090 Thermal Analyser system using platinum crucibles and alumina powder as a reference material. The stoichiometric combinations were mixed in isopropyl alcohol and dried in a stream of pure dry nitrogen just prior to use. Heating rates of $10^\circ C\,min^{-1}$ and cooling rates of $5^\circ C\,min^{-1}$ were used for all samples and extrapolated onset temperatures were determined for all recorded thermal events.

The intermediates of reaction were identified by room temperature X-ray diffraction analysis. Samples were heated at a rate of $5^\circ C\,min^{-1}$ and air-quenched at a variety of selected temperatures. The quenched samples were coated with plastic to prevent hydration of the species and were analysed using a Philips diffractometer. Intermediates were identified on the basis of X-ray diffraction peaks in the range 10°–50° 2θ.

3. Results and discussion

3.1. The raw materials

The melting points and/or phase transitions of the raw materials were investigated so that these thermal events could be separated from those corresponding to reactions in the binary, ternary and quaternary systems. The observed onset temperatures are summarized in Table I. It should be noted that the ZrO_2 tetragonal → monoclinic transition occurred between 950 and 1014° C depending on the thermal history of the sample [11]. Room temperature X-ray diffraction analysis of the trisodium phosphate sample indicated the presence of both α- and γ-phases in agreement with other workers [12–14].

3.2. Binary combinations

Observed onset temperatures for these systems are summarized in Table II. Thermal events corresponding to the phase transitions of the raw materials (Table I) have not been included.

3.2.1. $NH_4H_2PO_4$–Na_2CO_3

The solid-state reaction that occurs at $156 \pm 5^\circ C$ is so strongly endothermic that a negative slope is observed in DTA curves (Fig. 1b). The intermediates identified for this system were obtained from samples quenched from 175, 250, 620, 650 and 900° C. Viswanath and Miller [15, 16] report a high temperature phase transition of pure $NH_4H_2PO_4$ at $156 \pm 5^\circ C$. This suggests that the solid state reaction between $NH_4H_2PO_4$ and Na_2CO_3 may be facilitated by the phase change of $NH_4H_2PO_4$. Morey and Ingerson [17] report that $Na_5P_3O_{10}$ melts incongruently at 622° C to form crystalline sodium diphosphate and a melt of a mixture of $NaPO_3$ and $Na_4P_2O_7$ in a mole ratio of 0.505 : 0.495. This sharp melting is in agreement with DTA data observed in this study (Table II).

0022–2461/86 $03.00 + .12

TABLE I DTA results for raw materials used in the processing of Nasicon ceramics. Observed onset temperatures for heating cycle only

Material	Onset temperature ±5° C	Transition/melting/decomposition
$NH_4H_2PO_4$	199	$NH_4H_2PO_4 \rightarrow NH_3 + H_3PO_4$
	240	$2H_3PO_4 \rightarrow H_2O + H_4P_2O_7$
	290–300	$H_4P_2O_7 \rightarrow H_2O + 2HPO_3$
	> 300	sublimation of HPO_3
Na_2CO_3	70	dehydration
	356	$\gamma \rightarrow \beta$ phase transition
	483	$\beta \rightarrow \alpha$ phase transition
	858	melting
SiO_2	573	$\alpha \rightarrow \beta$ phase transition
	–	no quartz → tridymite transition observed
ZrO_2	1170	Monoclinic → tetragonal transition
Na_3PO_4	334	$\alpha \rightarrow \gamma$ phase transition

3.2.2. $NH_4H_2PO_4$–SiO_2

The DTA curve from 50–450° C for this system is shown in Fig. 1a. Samples quenched from 350, 450 and 600° C yielded highly viscous liquids containing quartz. The amount of quartz decreases with increase in the attained temperature. The products of reaction are amorphous.

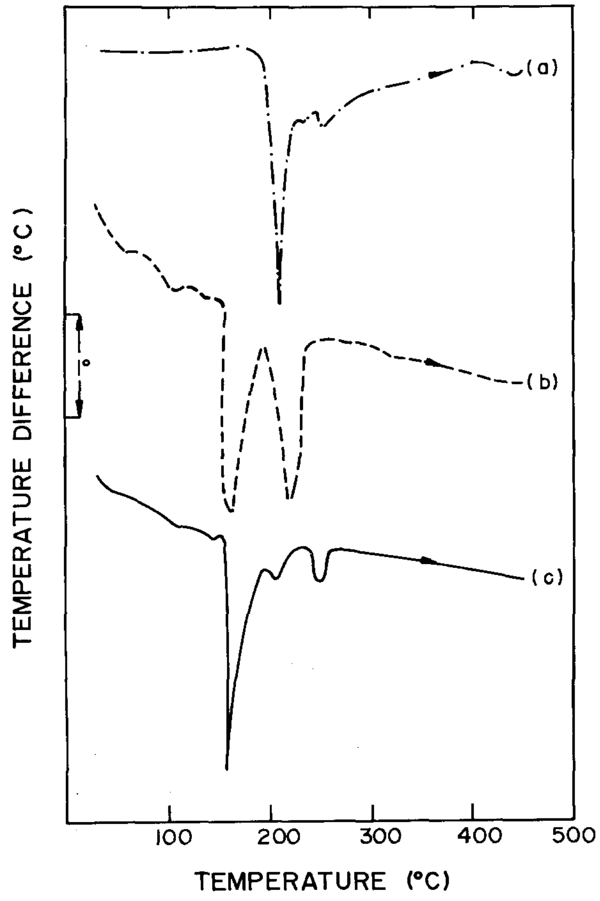

Figure 1 Differential thermal analysis curves of the systems (a) $NH_4H_2PO_4$–SiO_2; (b) $NH_4H_2PO_4$–Na_2CO_3; (c) $NH_4H_2PO_4$–Na_2CO_3–SiO_2 between 50° C and 450° C.

3.2.3. Na_2CO_3–SiO_2

X-ray diffraction analysis of a sample quenched at 765° C indicates the presence of Na_2SiO_3 although the exact onset of this reaction is not observed on DTA curves. Sodium disilicate $Na_2Si_2O_5$ is a minor reaction product in agreement with the phase diagram of Kracek [18]. The melting of sodium disilicate is observed at 775 ± 10° C. Due to higher mobility within the system, reactions leading to the formation of Na_2SiO_3 and $Na_2Si_2O_5$ are accelerated at temperatures above 775° C. The melting point of Na_2CO_3 is observed at 853 ± 5° C for samples containing large-grained Na_2CO_3. However, this melting is lowered to 814 ± 10° C for samples containing Na_2CO_3 of small particle size. This is in agreement with Wilburn and Thomasson [19]. Clear evidence of sodium volatilization from this system was observed [11] over the temperature range 770–880° C.

3.2.4. Na_2CO_3–ZrO_2

The DTA curve for this system is shown in Fig. 2. An endothermic reaction occurs over the wide temperature range between 507 ± 10° C and 1060 ± 10° C in agreement with Suzuki *et al.* [20]. Due to the proportion of components used unreacted ZrO_2 was observed in samples quenched at 1300° C.

3.2.5. SiO_2–ZrO_2

No reaction is observed up to 1300° C by DTA or X-ray diffraction analysis. This is in agreement with Curtis and Sowman [21] who established that the lower limit for synthesis of $ZrSiO_4$ is ~ 1314° C.

3.2.6. Na_3PO_4–SiO_2

A number of weak unidentifiable endotherms between 570 and 930° C indicate reactions between Na_3PO_4 and SiO_2. The products of reaction are amorphous. Sharp melting of the product(s) of reaction is observed at 935 ± 5° C. The melted product(s), which formed a glass on cooling, stabilized the high temperature γ–Na_3PO_4 phase to room temperature. In addition, the melt of the product(s) of reaction dissociated on cooling yielding γ-Na_3PO_4 or another glassy phase and α–cristobalite. This is in agreement with Turkdogan and Maddocks [22] although the thermodynamically stable compound $9Na_2O \cdot 2P_2O_5 \cdot 6SiO_2$ was not detected.

3.2.7. Na_3PO_4–ZrO_2

Reaction between Na_3PO_4 and ZrO_2 occurs in the solid state and yields an amorphous product. The exact onset of reaction could not be determined from DTA results.

3.3. Ternary combinations

Reactions that occur within these systems are summarized in Table III.

3.3.1. $NH_4H_2PO_4$–Na_2CO_3–SiO_2

Reactions up to 450° C closely correlate with those of the binary systems $NH_4H_2PO_4$–SiO_2 and $NH_4H_2PO_4$–Na_2CO_3 (see Fig. 1). The phosphoric acid produced at 195 ± 5° C may react with sodium carbonate or be taken up in the dissolution of quartz. The

TABLE 11 Summary of reactions identified in the binary systems

System	Onset temp ± 10° C	Reaction equation	Equation number	Comments
$NH_4H_2PO_4$–Na_2CO_3	50–150	$NH_4H_2PO_4 \rightarrow NH_3 + H_3PO_4$	2.1	slow decomposition followed by (2.2)
		$H_3PO_4 + Na_2CO_3 \rightarrow Na_2HPO_4 + CO_2 + H_2O$	2.2	acid–base reaction
	156	$NH_4H_2PO_4 + Na_2CO_3 \rightarrow Na_2HPO_4^* + CO_2 + NH_3 + H_2O$	2.3	strongly endothermic solid-state reaction
	196	$NH_4H_2PO_4 \rightarrow NH_3 + H_3PO_4$	2.4	melting and decomposition followed by (2.5)
		$H_3PO_4 + Na_3CO \rightarrow Na_2HPO_4^* + CO_2 + H_2O$	2.5	
	250	$2Na_2HPO_4^* \rightarrow Na_4P_2O_7^* + H_2O$	2.6	
	260–500	$2H_3PO_4 + Na_2CO_3 + 2Na_4P_2O_7^* \rightarrow 2Na_5P_3O_{10}^* + CO_2 + 3H_2O$	2.7a	series of weak endotherms. Either (2.7a) or (2.7b) or both reactions occur.
		$2NH_4H_2PO_4 + Na_2CO_3 + 2Na_4P_2O_7^* \rightarrow 2Na_5P_3O_{10}^* + CO_2 + 3H_2O + 2NH_3$	2.7b	
	624	melting of $Na_5P_3O_{10}^* \rightarrow Na_4P_2O_7^*$ + melt of $(Na_4P_2O_7 + NaPO_3)$	2.8	reference [17]
	700	$Na_4P_2O_7^* + Na_2CO_3 \rightarrow 2Na_3PO_4^* + CO_2$	2.9	mixture of α- and γ-Na_3PO_4 identified
$NH_4H_2PO_4$–SiO_2	191	$NH_4H_2PO_4 \rightarrow NH_3 + H_3PO_4$	2.10	melting and decomposition. Rapid progressive dissolution of SiO_2 into liquid H_3PO_4
	230†		2.11	
	413	→ amorphous product(s)	2.12	
	450†		2.13	
Na_2CO_3–SiO_2	< 765	$SiO_2 + Na_2CO_3 \rightarrow Na_2SiO_3^*$	2.14	onset not evident on DTA. Solid state reaction.
	< 775	$SiO_2 + Na_2SiO_3^* \rightarrow Na_2SiO_5^*$	2.15	minor reaction
	775	melting of Na_2SiO_5	2.16	(2.14) and (2.15) accelerated
	853	melting of Na_2CO_3	2.17	(2.14) and (2.15) accelerated. Melting point lowered to 814° C for small Na_2CO_3 particle size.
Na_2CO_3–ZrO_2	507–1060	$3Na_2CO_3 + 3ZrO_2 \rightarrow 3Na_2ZrO_3^* + 3CO_2 + ZrO_2^*$	2.18	wide endotherm. Unreacted ZrO_2 expected
	824	melting of Na_2CO_3	2.19	(2.18) accelerated
ZrO_2–SiO_2	–	no reaction up to 1300° C		reference [20]
Na_3PO_4–SiO_2	570–930	$Na_3PO_4 + SiO_2 \rightarrow$ amorphous product	2.20	series of weak endotherms
	935	melting of $(Na_3PO_4$–$SiO_2)$ product	2.21	
Na_3PO_4–ZrO_2	< 1170	$Na_3PO_4 + ZrO_2 \rightarrow$ amorphous product	2.22	onset not evident on DTA. Slow solid-state reaction. Complete by 1170° C.

*Intermediates/products identified by X-ray diffraction analysis.

†Exothermic reactions (all other reactions are endothermic).

TABLE III Summary of reactions identified in the ternary systems

System	Onset temp ± 10° C	Reaction equation	Equation number	Comments
$NH_4H_2PO_4$–Na_2CO_3–SiO_2	50–150	$NH_4H_2PO_4 \rightarrow NH_3 + H_3PO_4$	2.1	
		$H_3PO_4 + Na_2CO_3 \rightarrow Na_2HPO_4 + H_2O + CO_2$	2.2	
	158	$NH_4H_2PO_4 + Na_2CO_3 \rightarrow Na_2HPO_4 + CO_2 + NH_3 + H_2O$	2.3	
	195	$NH_4H_2PO_4 \rightarrow NH_3 + H_3PO_4$	2.4	
		$H_3PO_4 + Na_2CO_3 \rightarrow Na_2HPO_4 + CO_2$	2.5	competition for H_3PO_4
		dissolution of SiO_2 in H_3PO_4	2.11	
	250–600	$2Na_2HPO_4 \rightarrow Na_4P_2O_7 + H_2O$	2.6	
		$2H_3PO_4 + Na_2CO_3 + 2Na_4P_2O_7 \rightarrow 2Na_5P_3O_{10} + CO_2 + 3H_2O$	2.7a	H_3PO_4 from 2.11
		$2NH_4H_2PO_4 + Na_2CO_3 + 2Na_4P_2O_7 \rightarrow 2Na_5P_3O_{10} + CO_2 + 3H_2O + 2NH_3$	2.7b	for $NH_4H_2PO_4$ unreacted prior to this reaction
	615	melting of $Na_5P_3O_{10} \rightarrow Na_4P_2O_7$ + melt of $(Na_4P_2O_7 + NaPO_3)$	2.8	
	760–800	$Na_4P_2O_7 + Na_2CO_3 \rightarrow 2Na_3PO_4^* + CO_2$	2.9	competition for remaining Na_2CO_3. Possible volatilization of Na_2O
		$Na_2CO_3 + SiO_2 \rightarrow Na_2^*SiO_3 + CO_2$	2.14	
	845	melting of Na_2CO_3	2.17	change in slope observed. Trace of Na_2CO_3 only liquid at this temperature
	900	$Na_4P_2O_7 + Na_2SiO_3 \rightarrow$ amorphous product(s)	3.1	
	800–930	$Na_3PO_4 + SiO_2 \rightarrow$ amorphous product(s)	2.20	
	934	melting of $(Na_3PO_4$–$SiO_2)$ product	2.21	
Na_2CO_3–SiO_2–ZrO_2	< 770	$SiO_2 + Na_2CO_3 \rightarrow Na_2SiO_3$	2.14	onset not evident on DTA
		$SiO_2 + Na_2SiO_3 \rightarrow Na_2Si_2O_5$	2.15b	minor reaction. Melting at 775 ± 10° C
	815	melting of Na_2CO_3	2.17	(2.14) and (2.15) accelerated
	< 1000	dissolution of ZrO_2 in Na_2SiO_3 and $Na_2Si_2O_5 \rightarrow Na_4Zr_2Si_3O_{12}^*$	3.2	ZrO_2^* and $Na_2SiO_3^*$ remain. Onset not evident on DTA. Rate-determining step.
Na_3PO_4–SiO_2–ZrO_2	600–1000	$Na_3PO_4 + ZrO_2 \rightarrow$ amorphous $(Na_3PO_4$–$ZrO_2)$ intermediate	2.22	slow. Onset not evident on DTA. Minor reaction
	570–930	$Na_3PO_4 + SiO_2 \rightarrow$ amorphous $(Na_3PO_4$–$SiO_2)$ intermediate	2.20	
	800–1000	$(Na_3PO_4$–$ZrO_2)$ intermediate $+ SiO_2 \rightarrow Na_3Zr_2Si_2PO_{12}$	3.3	rapid formation especially after (3.4)
	935	melting of $(Na_3PO_4$–$SiO_2)$ intermediate	3.4	
	900–1200+	dissolution of ZrO_2 in $(Na_3PO_4$–$SiO_2)$ intermediate to form $Na_3Zr_2Si_2PO_{12}$	3.5	rate-determining step(s)
	1300	incongruent melting of $Na_3Zr_2Si_2PO_{12}$	3.6	

*Species identified by X-ray diffraction analysis.

TABLE IV Summary of reactions identified in the $NH_4H_2PO_4$–Na_2CO_3–SiO_2–ZrO_2 system

Onset temp ± 10° C	Reaction equation	Equation number	Comments
25–150	$NH_4H_2PO_4 \rightarrow NH_3 + H_3PO_4$	2.1	
	$H_3PO_4 + Na_2CO_3 \rightarrow Na_2HPO_4 + H_2O + CO_2$	2.2	
154	$NH_4H_2PO_4 + Na_2CO_3 \rightarrow Na_2HPO_4 + CO_2 + NH_3 + H_2O$	2.3	
200	$NH_4H_2PO_4 \rightarrow NH_3 + H_3PO_4$	2.4	
	$H_3PO_4 + Na_2CO_3 \rightarrow Na_2HPO_4 + CO_2$	2.5	
	dissolution of SiO_2 and ZrO_2 in H_3PO_4	2.11	exothermic, reversible
244	$2Na_2HPO_4 \rightarrow Na_4P_2O_7 + H_2O$	2.6	
250–600	$2H_3PO_4 + Na_2CO_3 + 2Na_4P_2O_7 \rightarrow 2Na_5P_3O_{10} + CO_2 + 3H_2O$	2.7a	H_3PO_4 from 2.11
	$2NH_4H_2PO_4 + Na_2CO_3 + 2Na_4P_2O_7 \rightarrow 2Na_5P_3O_{10} + CO_2 + 3H_2O + 2NH_3$	2.7b	for $NH_4H_2PO_4$ unreacted prior to this reaction
613	melting of $Na_5P_3O_{10} \rightarrow Na_4P_2O_7$ + melt of $(Na_4P_2O_7 + NaPO_4)$	2.8	
760–800	$Na_4P_2O_7 + Na_2CO_3 \rightarrow 2Na_3PO_4 + CO_2$	2.9	competition with (2.14) for remaining Na_2CO_3
	$Na_3PO_4 + ZrO_2 \rightarrow$ amorphous product(s)	2.22	onset of solid-state reaction
	$Na_3PO_4 + SiO_2 \rightarrow$ amorphous product(s)	2.20	onset of solid-state reaction
	$Na_2CO_3 + SiO_2 \rightarrow Na_2SiO_3 + CO_2$	2.14	possible volatilization of Na_2O
	$Na_2SiO_3 + SiO_2 \rightarrow Na_2Si_2O_5$	2.15–6	minor reaction, melting at 775 ± 10° C
800	formation of $Na_4Zr_2Si_3O_{12}$	3.2	slow reaction
900	$Na_4P_2O_7 + Na_2SiO_3 \rightarrow$ amorphous product(s)	4.1	minor reaction
935	melting of $(Na_3PO_4$–$SiO_2)$ intermediate	3.4	higher mobility in the system
< 1000	$(Na_3PO_4$–$ZrO_2)$ intermediate $+ SiO_2 \rightarrow Na_3Zr_2Si_2PO_{12}$	4.2	reaction complete by 1000° C
1014	$(Na_3PO_4$–$SiO_2)$ intermediate $+ ZrO_2 \rightarrow Na_3Zr_2Si_2PO_{12}$	4.3	rate-determining step
	$(Na_4P_2O_7$–$Na_2SiO_3)$ intermediate $+ ZrO_2 \rightarrow Na_3Zr_2Si_2PO_{12}$	4.4	minor reaction
	$Na_4Zr_2Si_3O_{12} + NaZr_2P_3O_{12} \rightarrow 2Na_3Zr_2Si_2PO_{12}$	4.5	minor reaction, solid solution
1302	incongruent melting of $Na_3Zr_2Si_2PO_{12}$	3.6	

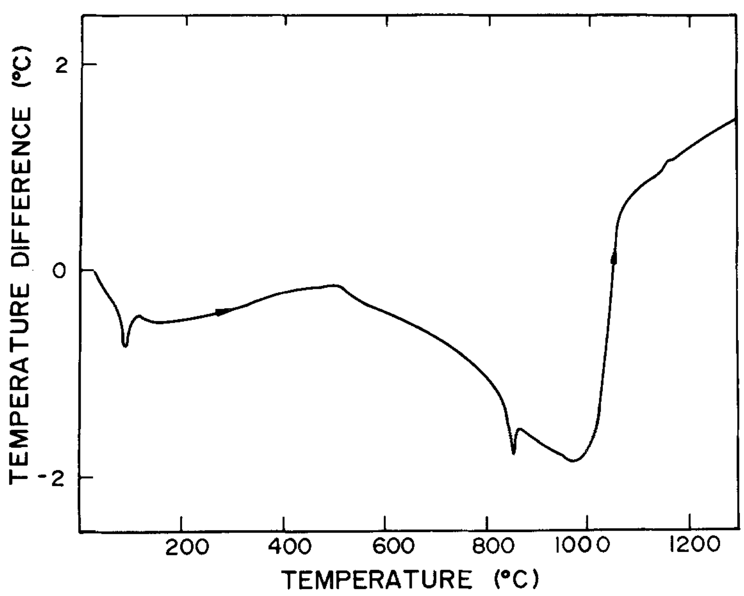

Figure 2 Differential thermal analysis curve of the sodium carbonate–zirconia system (molar ratio 3:4).

latter process is reversible and at higher temperatures (Equation 2.7a, Table III) quartz precipitates as the phosphoric acid reacts further with Na_2CO_3 and $Na_4P_2O_7$ to form sodium tripolyphosphate [11]. It should be noted that at temperatures above 845° C the system becomes mobile due to the presence of liquid phases. All products of reaction are amorphous.

3.3.2. Na_2CO_3–SiO_2–ZrO_2

Reactions up to 820° C closely correlate with the Na_2CO_3–SiO_2 system. The onset of formation of $Na_4Zr_2Si_3O_{12}$ was not observed on DTA traces. X-ray diffraction analysis of a sample quenched at 1000° C indicates the presence of $Na_4Zr_2Si_3O_{12}$, Na_2SiO_3 and ZrO_2. Several unidentified peaks were observed. These are ascribed to intermediates in the process of dissolution of ZrO_2 in the sodium silicates. This process is the rate determining step of reaction and is dependent on the particle size of ZrO_2. The alternative reaction route in the formation of $Na_4Zr_2Si_3O_{12}$ occurs via the sodium metazirconate intermediate (Equation 2.18, Table II) followed by dissolution of SiO_2. However, no evidence from DTA or X-ray diffraction analysis was observed for the formation of Na_2ZrO_3 in the ternary system.

3.3.3. Na_3PO_4–SiO_2–ZrO_2

The formation of Nasicon of formula $Na_3Zr_2Si_2PO_{12}$ occurs via two competitive routes. Firstly, Na_3PO_4 and ZrO_2 react to form an amorphous intermediate (Table III) followed by dissolution of SiO_2 to form Nasicon. Nasicon formation via this route is complete by 1000° C. In the second competitive route Na_3PO_4 and SiO_2 react to form an amorphous intermediate in which ZrO_2 dissolves to form Nasicon. The dissolution of ZrO_2 in the (Na_3PO_4–SiO_2) intermediate is the rate determining step and is dependent on the particle size of ZrO_2. The dissolution process occurs in several stages. Since ZrO_2 and Nasicon were identified in a sample quenched at 1200° C a kinetic hindrance to completeness of reaction is implied.

3.4. Four-component system

3.4.1. $Na_2H_2PO_4$–Na_2CO_3–SiO_2–ZrO_2

Many of the DTA peaks for this system were not sharp enough to be accurately determined. The complete reaction sequence given in Table IV was deduced from reactions identified in the binary and ternary systems. Formation of Nasicon via the (Na_3PO_4–ZrO_2) intermediate is essentially complete by 1000° C although this reaction route is minor. Nasicon formation via the (Na_3PO_4–SiO_2) intermediate followed by dissolution of ZrO_2 is the major reaction route. The dissolution of ZrO_2 again is the rate-determining step and occurs in several stages of the reaction. Complete reaction was not achieved.

4. Conclusions

Partial reactions and intermediates within the $NH_4H_2PO_4$–Na_2CO_3–SiO_2–ZrO_2 and Na_3PO_4–SiO_2–ZrO_2 systems have been identified. In both the three- and four-component systems the major reaction route is via a sodium phosphosilicate intermediate that is liquid at the formation temperature of Nasicon. ZrO_2 dissolves in the sodium phosphosilicate intermediate to form Nasicon. Second phase ZrO_2 material was detected after reaction in the three- and four-component systems. The rate-determining step in both systems is the dissolution of ZrO_2 in the (liquid) sodium phosphosilicate intermediate. Kinetic restrains in the traditional processing of Nasicon are therefore indicated from mixtures containing ZrO_2 as a starting material. Na_2O volatilization occurs in the Na_2CO_3–SiO_2 system and at the adopted heating rate of 10° C min^{-1} may occur in the four-component system.

References

1. H. Y-P. HONG, *Mater. Res. Bull.* **11** (1976) 173.
2. J. B. GOODENOUGH, H. Y.-P. HONG and J. A. KAFALAS, *ibid.* **11** (1976) 203.
3. M. L. BAYARD and G. G. BARNA, *J. Electroanal. Chem.* **91** (1978) 201.
4. J. P. BOILOT, J. P. SALANIÉ, G. DESPLANCHES and D. LE POTIER, *Mater. Res. Bull.* **14** (1979) 1469.
5. J. A. KAFALAS and R. J. CAVA, in "Fast Ion Transport in Solids", edited by P. Vashishta, J. N. Mundy and G. K. Shenoy (North-Holland, Amsterdam, 1979) p. 419.
6. G. DESPLANCHES, M. RIGAL and A. WICKER, *Ceram. Bull.* **59** (1980) 546.
7. G. R. MILLER, B. J. McENTIRE, T. D. HADNAGY, J. R. RASMUSSEN and R. S. GORDON, in "Fast Ion

Transport in Solids", edited by P. Vashishta, J. N. Mundy and Transport in Solids", edited by P. Vashishta, J. N. Mundy and G. K. Shenoy (North-Holland, Amsterdam, 1979) p. 83.

8. D. H. H. QUON, T. A. WHEAT and W. NESBITT, *Mater. Res. Bull.* **15** (1980) 1533.
9. B. J. McENTIRE, R. A. BARTLETT, G. R. MILLER and R. S. GORDON, Department of Energy Contract no. E1-78-C-01-5162. Report for Subcontract no. 4507310.
10. M. PORTHAULT and J.-C. MERLIN, *Compt. Rend.* **246** (1958) 2763.
11. V. A. NICHOLAS, MSc thesis, University of South Africa, 1985.
12. M. PALAZZI and F. RÉMY, *Bull. Soc. Chim. Fr.* **8** (1971) 2795.
13. A-W. KOLSI, *Rev. Chim. Miner.* **13** (1976) 416.
14. VON D. M. WIENCH and M. JANSEN, *Z. Anorg. Allg. Chem.* **461** (1980) 101.
15. R. S. VISWANATH and P. J. MILLER, *Solid State Commun.* **29** (1979) 163.
16. *Idem, ibid.* **32** (1979) 703.
17. G. W. MOREY and E. INGERSON, *Amer. J. Sci.* **242** (1944) 1.
18. F. C. KRACEK, *J. Amer. Chem. Soc.* **61** (1939) 2869.
19. F. W. WILBURN and C. V. THOMASSON, *J. Glass Technol.* **42** (1958) 158T.
20. H. SUZUKI, S. KIMURA, H. YAMADA and T. YAMAUCHI, *J. Jpn. Ceram. Soc.*, **69** (1961) 52.
21. C. E. CURTIS and H. G. SOWMAN, *J. Amer. Ceram. Soc.* **36** (1953) 190.
22. E. T. TURKDOGAN and W. R. MADDOCKS, *J. Iron Steel Inst.* **172** (1952) 1.

Received 7 June
and accepted 5 August 1985